Available online at www.sciencedirect.com
ScienceDirect
Journal of Catalysis 252 (2007) 161–170
JOURNAL OF CATALYSIS
www.elsevier.com/locate/jcat

Isomerization of α-pinene over dealuminated ferrierite-type zeolites

Rafal Rachwalik [a], Zbigniew Olejniczak [b], Jian Jiao [c], Jun Huang [c], Michael Hunger [c], Bogdan Sulikowski [a,*]

[a] *Institute of Catalysis and Surface Chemistry, Polish Academy of Sciences, Kraków, Poland*
[b] *Institute of Nuclear Physics, Polish Academy of Sciences, Kraków, Poland*
[c] *Institute of Chemical Technology, University of Stuttgart, Stuttgart, Germany*

Received 30 May 2007; revised 26 September 2007; accepted 2 October 2007

Abstract

Isomerization of α-pinene was performed on a series of dealuminated ferrierite (FER)-type zeolites in liquid phase at 363 K using a batch reactor. The course of zeolite dealumination was followed in detail using ^{29}Si, ^{27}Al, ^{1}H MAS NMR, XRD, FTIR, and sorption of nitrogen. The ammonium form of FER was dealuminated with aqueous solutions of HCl. While retaining the crystallinity of the zeolite particles, the treatments removed up to 53% of the tetrahedrally coordinated aluminum atoms from the FER framework. According to ^{29}Si MAS NMR studies, the framework aluminum atoms located at the 10-membered rings in the main channels of FER (T_B sites) were depleted preferentially from their positions. Even relatively mild dealumination of FER led to an active catalyst containing both Brønsted and Lewis centers, yielding up to 97% conversion of α-pinene at 363 K, in contrast to the 72% observed for the parent hydrogen form. Such catalytic behavior was discussed in terms of the conversion of a reactant inside micropores of the zeolite catalyst, on Brønsted acid centers with enhanced strength located probably in the vicinity of Lewis sites. The selectivity toward camphene and limonene changed smoothly with the dealumination level; thus, a higher selectivity toward limonene was observed at the expense of camphene formation with increasing the n_{Si}/n_{Al} ratio of the catalysts. The selectivity toward camphene and limonene was close to 85% for all of the materials studied. The initial rates of α-pinene transformations over FER-type materials exceeded those observed for other catalytic systems, heteropoly acid/SiO_2 and H_2SO_4/ZrO_2. This study demonstrates the successful application of a medium-pore zeolite for the catalytic transformation of α-pinene in liquid phase.

Keywords: Ferrierite; Dealumination; Isomerization of α-pinene; ^{1}H, ^{27}Al and ^{29}Si MAS NMR; FTIR

1. Introduction

Renewable resources are becoming increasingly important for producing a variety of fine and bulk chemicals. Terpene feedstocks are some of these raw materials. Of these, the *alfa* and *beta* isomers of pinene are used to manufacture a number of products for the pharmaceutical and chemical industries [1]. The isomerization of α-pinene, catalyzed by acid centers, is of industrial significance. It gives bicyclic products, exemplified by camphene, and monocyclic products such as limonene and *p*-cymene (Scheme 1) [2–4]. Camphene is an intermediate compound for producing isoborneol, isobornyl acetate, and camphor [5].

Various acidic catalysts, such as oxides treated with acids [6,7], modified zeolites [4,8–10], activated clays [11,12], and heteropoly acids [13–15], have been suggested in the literature for the isomerization of α-pinene (Scheme 1). Basic catalysts have been reported for isomerization of α- to β-pinene (alkaline earth-metal oxides [16] and calcium amide [17]). Currently, the main method for camphene production is based on the isomerization of α-pinene in the presence of the weakly acidic hydrated TiO_2 catalyst [18].

In the present work, a medium-pore zeolite ferrierite (FER) was chosen as the catalyst. FER, with slightly smaller pore openings than ZSM-5 (MFI), is seldom found in nature. It is produced on an industrial scale. FER is quite distinct from most known zeolites as the four-membered rings are not present in its structure. Its topological density, N_1–N_{10}, is high (1021) compared with other zeolites [19]. Its structure

* Corresponding author. Fax: +48 12 4251923.
E-mail address: ncsuliko@cyf-kr.edu.pl (B. Sulikowski).

0021-9517/$ – see front matter
doi:10.1016/j.jcat.2007.10.001

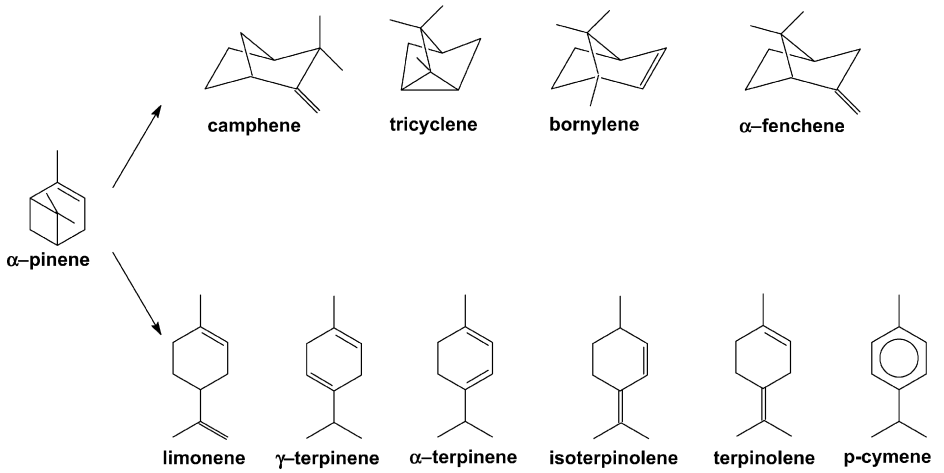

Scheme 1. Products given by isomerization of α-pinene over dealuminated ferrierite-type zeolites.

is stable against thermal, hydrothermal, and chemical treatments.

The objectives of the present work were to provide a detailed account of FER dealumination by hydrochloric acid, using ^{29}Si, ^{27}Al and ^{1}H MAS NMR in tandem with FTIR, and to study isomerization of α-pinene catalyzed by the materials obtained. The results allowed a comparison of the performance of FER samples in relation to a heteropoly acid and sulfated zirconium oxide.

2. Experimental

2.1. Preparation of the samples

The ammonium form of labeled NH_4-T was dealuminated with aqueous solutions of hydrochloric acid applying a multistep procedure. First, NH_4-T was obtained by an ion-exchange of a zeolite, K,Na-FER, purchased from Tosoh, Japan ($n_{Si}/n_{Al} = 9.2$). The ion-exchange process was repeated four times using a 0.5 M aqueous solution of ammonium nitrate at room temperature for 12 h. The NH_4-exchanged sample was washed and dried at 373 K overnight. The material thus obtained was calcined at 773 K for 5 h to yield the hydrogen form H-FER (T0), used as a reference catalyst. The parent zeolite NH_4-T was dealuminated by a multistep procedure. First, a 100-g portion of zeolite NH_4-T was treated with 0.25 M HCl solution at 368 K for 4 h, washed until no Cl^- ions could be detected in the solution, and dried at 373 K overnight (step 1). The resultant sample, T1, was dealuminated further applying the same procedure, but with the HCl concentration in solution progressively increased in consecutive steps, that is, 0.25 M (step 1) to 1.0 M (step 2) and, finally, to 2.0 M HCl (step 3). The treatments with acid in the second and third steps were carried out at ambient temperature to yield samples labeled T2 and T3.

2.2. XRD measurements

Powder X-ray diffraction (XRD) patterns of the hydrated samples for 2θ ranging from 5 to 50° were recorded on a Siemens D5005 automatic diffractometer with CuK_α radiation. Silicon powder was used as the internal standard in a quantity of 15 wt% for calibrating the diffraction angle and estimating the crystallinity of the parent and dealuminated materials.

2.3. Sorption properties

Sorption of nitrogen was studied using the Quantachrome Autosorb automated gas sorption system. Before the measurements, the samples were outgassed at 473 K for 24 h. The external surface area (S_E), internal surface area (S_μ), total pore volume (V_T), and micropore volume (V_μ) were determined by applying the t-method micropore analysis according to de Boer. SiO_2 was used as the reference material.

Adsorption of α-pinene was studied using potassium forms of the starting sample and the most dealuminated one. Four-fold ion exchange with 0.5 M KNO_3 solution was applied at 353 K for 2 h each to yield the samples labeled K-T0 and K-T3, respectively. The samples were loaded into the two GC columns and outgassed at 723 K for 1 h before the measurements. Adsorption of α-pinene was studied using a gas chromatographic method at 453 K, because the boiling point of α-pinene is 429 K.

2.4. MAS NMR measurements

^{29}Si MAS NMR spectra were recorded on a homemade NMR spectrometer at the magnetic field of 7.05 T using single-pulse excitation of 4 μs ($\pi/2$), a repetition time of 10 s, and a sample spinning rate of 4 kHz. ^{1}H and ^{27}Al MAS NMR spectra were measured using a Bruker MSL-400 spectrometer at a magnetic field of 9.4 T, with single-pulse excitations of 2.2 μs ($\pi/2$) and 0.6 μs ($\pi/2$), and repetition times of 30 and 0.5 s, respectively; 160 and 1024 scans, respectively, were acquired at a spinning rate of ca. 8.0 kHz. Decomposition and simulation of the NMR spectra were performed using the Bruker WINNMR and WINFIT software.

^{27}Al and ^{29}Si MAS NMR investigations were performed on fully hydrated samples. For this purpose, the samples were exposed to the vapor of a saturated $Ca(NO_3)_2$ solution at ambient temperature for 12 h. The ^{27}Al MAS NMR spectra were

normalized taking into account the acquisition numbers and the sample mass. For the quantitative evaluation, the signal intensities of the tetrahedrally coordinated framework aluminum atoms occurring at ca. 60 ppm were compared with that of the well-defined parent material T0.

Before the ^{1}H MAS NMR experiments, the samples were dehydrated at 723 K for 12 h in a vacuum of $p < 10^{-6}$ Pa, and then filled into 4-mm MAS rotors in a glove box purged with dry nitrogen. Quantitative ^{1}H MAS NMR studies were performed using normalized spectra and comparing the signal intensities with that of an external intensity standard. The standard sample was a dehydrated zeolite H,Na-Y (exchange degree, 35%) with 1.776 mmol OH groups/g and a weight of 58.5 mg.

2.5. FTIR spectroscopy

FTIR measurements (for adsorption of both ammonia and CO) were performed on self-supported discs of zeolites (about 10 mg/cm^2) on a Bruker 48 PC spectrometer equipped with an MCT detector and with a spectral resolution of 2 cm^{-1}. In the most cases, 100–200 scans were recorded. FER samples were activated in situ in the IR cell at 803 K for 2 h under a vacuum of $p < 10^{-6}$ Pa. Concentration of Brønsted acid sites was determined by adsorption of ammonia, using a 1450-cm^{-1} band of ammonium ions and an extinction coefficient of 14.8 cm/μmol.

The strength of acid sites was estimated by NH_3 thermodesorption and CO adsorption. Thus the ratios of the integral intensity of the IR band of chemisorbed ammonium ions at 1450 cm^{-1} for the samples calcined at 650 K (A_{650}) and 453 K (A_0) were evaluated. The adsorption of CO was performed and studied at the temperature of liquid nitrogen.

FTIR spectra were normalized, taking into account specific density of a self-supported wafer.

2.6. Catalytic studies

The conversion of α-pinene was carried out at atmospheric pressure in a batch-type glass reactor equipped with a reflux condenser, a stirrer, and a temperature controller. In a typical run, 20 mL of α-pinene (Fluka) was heated to 363 K. The catalyst (1.0 g) was calcined at 673 K for 5 h in a helium flow, cooled in He to ambient temperature, and then added to the reaction mixture. The reaction was carried out under isothermal conditions at 363 K. After selected times, 10-μL aliquots of the reaction mixture were obtained for GC analysis. The reaction products were analysed by an HP 6890 gas chromatograph equipped with a thermal conductivity detector, a homemade packed column (3 m, 2.0 mm i.d., with 8% bentone-34, 6% didecyl phthalate, and 1% silicon oil A on Chromosorb W) [20].

3. Results and discussion

3.1. Dealumination of FER

The n_{Si}/n_{Al} ratio in zeolites is of paramount importance for catalysis, because the number and strength of the Brønsted acid centers are governed strictly by the number of framework aluminum atoms [21]. Numerous dealumination methods have been developed to vary the composition of the zeolite framework at will [22]. One of these methods is based on the use of mineral acids. When considering such a treatment of any aluminosilicate, the major factor is the framework's resistance to acid. Some zeolites are not stable even against mild acids; thus, our first concern was the stability of the zeolite framework under treatment with hydrochloric acid of different concentration. Detailed inspection of the XRD diffraction patterns of the FER-type samples after dealumination revealed neither collapse of the zeolite framework nor any significant change in the integrity of the zeolite crystals. Only small and anisotropic unit cell contractions did occur during this treatment, producing pronounced shifts of the reflections characteristic of atoms arranged along the a-axis of the unit cell. This is in accordance with our earlier study of this type of zeolite, albeit of a different origin (Zeolyst) [23].

Table 1
Sorption properties of the reference sample T0 (H-FER) in comparison with the dealuminated materials (T1–T3) as determined by nitrogen adsorption

Sample	SSA[a] (m^2/g)	S_E[b] (m^2/g)	S_μ[c] (m^2/g)	V_T[d] (cm^3/g)	V_μ[e] (cm^3/g)	V_m[f] (cm^3/g)
T0 (H-FER)	275	40	235	0.243	0.129	0.114
T1	300	39	261	0.300	0.134	0.166
T2	299	41	258	0.277	0.133	0.144
T3	278	45	233	0.358	0.120	0.238

[a] SSA—specific surface area.
[b] S_E—external surface area.
[c] S_μ—internal surface area.
[d] V_T—total pores volume.
[e] V_μ—micropores volume.
[f] V_m—mesopores volume (comprises mesopores volume + intercrystalline space between ferrierite crystals).

Sorption studies of nitrogen on the parent and dealuminated samples are summarized in Table 1. The specific surface areas were essentially the same for all of the samples under study. The micropore volume was largely retained even after the third dealumination step, that is, 0.129 and 0.120 cm^3/g for samples T0 and T3, respectively. In addition, pores in the mesopore range (Table 1, last column) started to develop slightly after mild treatment with HCl; however, this increase was not significant for the T1 and T2 samples. Only after using 2 M HCl did the sample contain twice the amount of mesopores as the parent sample T0. The acid solution removes some aluminum atoms from framework position and washes them out of the pore system, leading to the formation of secondary pores in the mesopore range (vide infra). However, the average crystals size is not affected by dealumination with HCl (SEM, not shown), thus supporting earlier findings [24].

To acquire information on α-pinene sorption on FER, adsorption of the reactant was carried out by gas chromatography. Because the isomerization of sorbate proceeds at 363 K, the hydrogen forms of the samples could not be used. Instead, the potassium-exchanged forms of the starting material and of the most dealuminated material were prepared, thereby avoiding catalytic transformations of α-pinene during the experiment.

Sorption was studied at 453 K. (The boiling point of α-pinene is 429 K.) The amount of α-pinene adsorbed on the potassium form K-T0 was 88 mg/g; this increased to 109 mg/g on the most dealuminated sample, K-T3. Note the large difference in diameter between H^+ and K^+ ions; sorption on the hydrogen forms in fact would be higher.

^{29}Si and ^{27}Al MAS NMR spectroscopy was used to study the location and chemical surroundings of silicon and aluminum atoms in the parent and dealuminated zeolites. The exact distribution of silicon and aluminum in the framework gives rise to physical and chemical properties of the solid, with sorptive and catalytic properties likely to be the most important for applications. For example, the siting of Brønsted acid centers, required for the overwhelming majority of reactions catalyzed by zeolites, is inherently connected with the aluminum distribution at the T sites. Whereas ^{29}Si MAS NMR spectroscopy gives the distribution of tetrahedrally coordinated silicon atoms with different numbers of aluminum atoms or hydroxyl groups in their vicinity, quantitative estimation of the distribution of aluminum between framework and non-framework positions is a major concern in the ^{27}Al NMR spectroscopy in zeolites.

Estimation of Al location at the framework/non-framework zeolite positions is by no means straightforward, because Al is a quadrupolar nuclei with spin of 5/2. In faujasite series, for example, the values for the non-framework aluminum were consistently lower than those obtained from the silicon spectra, and the presence of so called "invisible aluminum" in zeolites has been reported [25,26]. The amounts of framework and non-framework aluminum can be estimated correctly provided that certain experimental conditions are met [27]. First, the samples must be fully hydrated. Second, the radiofrequency pulses must be short; otherwise, a considerable loss of spectral intensity leads to serious underestimation of the aluminum in the samples. Al in a highly distorted coordination might become NMR-silent. Thus, quantitative measurements were performed with fully hydrated samples, and only the signals of the well-defined tetrahedrally coordinated Al species were evaluated.

Fig. 1 shows the ^{27}Al MAS NMR spectra of all the samples, in which signals at ca. 54 ppm are attributed to tetrahedrally coordinated framework aluminum atoms. In the spectra of the dealuminated zeolites, the signal at 0 ppm indicates the presence of a small number of octahedrally coordinated extra-framework aluminum species, possibly acting as Lewis acid sites. For the reference sample T0 (H-FER), a strong signal at 54 ppm and a very weak signal at 0 ppm indicate that nearly all the aluminum atoms are tetrahedrally coordinated in the framework. The intensity of this signal decreases stepwise on treatment with hydrochloric acid solutions; the dealumination levels calculated from ^{27}Al NMR spectra are given in Table 2, last column. For more strongly dealuminated materials, such as samples T2 and T3, the signal of tetrahedrally coordinated aluminum atoms is broadened (high-field shoulder). This indicates that some of the framework aluminum atoms in the dealuminated materials exhibit lower symmetry, thus giving rise to a distorted local structure.

In the case of FER-type zeolites, the ^{29}Si MAS NMR spectra are a superposition of signals due to silicon atoms at the crystallographically nonequivalent positions T_A and T_B. Takaishi et al. [28] proposed a model of the distribution of aluminum atoms (6 Al per unit cell) in the FER framework depicted in Scheme 2. According to this model, the framework aluminum atoms are located at the crystallographic positions labeled $T_{1,1}$, $T_{1,10}$, $T_{2,1}$, $T_{2,2}$, $T_{2,4}$, and $T_{2,9}$. There are 3.6 Al/uc in the reference sample T0 (Table 2, columns 4 and 5). This situation was represented in Scheme 2 by considering 4 Al/uc. The silicon atoms at the aforementioned positions T_A and T_B are located in the neighborhood of framework aluminum atoms located at $T_{1,1}$, $T_{1,10}$, $T_{2,2}$, and $T_{2,11}$ or $T_{1,1}$, $T_{1,10}$, $T_{2,4}$, and $T_{2,9}$ positions, respectively (Schemes 2a and 2b).

The ^{29}Si MAS NMR spectrum of the ammonium form NH_4-T consists of four signals at −105.0, −109.0, −115.5, and −112.0 ppm due to Si(1Al) T_A, Si(1Al) T_B, Si(0Al) T_B, and Si(0Al) T_A species, respectively (Fig. 2a). An additional ^{29}Si MAS NMR signal at −103 ppm is attributed to Q^3 silicon atoms (SiOH) at framework defects or the outer surface of the zeolite particles [29].

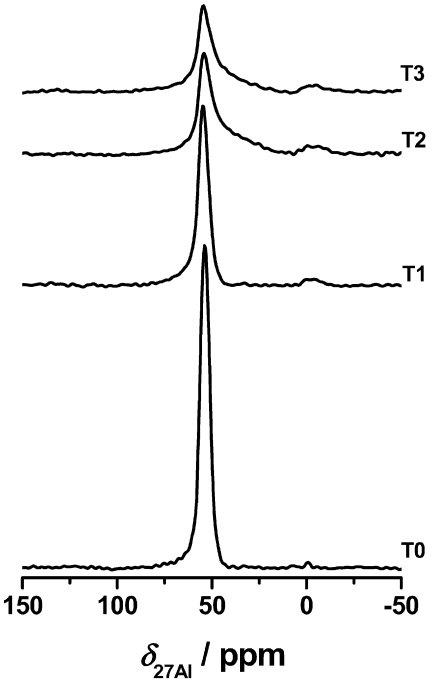

Fig. 1. Monocyclic, bicyclic and tricyclic products given by isomerization of α-pinene.

Table 2
A comparison of the n_{Si}/n_{Al} ratios and numbers of aluminum atoms, N_{Al}, determined by elemental analysis and ^{29}Si and ^{27}Al MAS NMR spectroscopy, for the parent T0 (H-FER) and dealuminated samples T1–T3

Sample	n_{Si}/n_{Al}		N (Al/uc)		Dealumination (%)	
	Bulk[a]	NMR[b]	Bulk[a]	NMR[b]	^{29}Si NMR[b]	^{27}Al NMR[c]
T0 (H-FER)	8.9	9.1	3.6	3.6	0	0
T1	12.5	12.6	2.7	2.6	38	30
T2	17.1	18.2	2.0	1.9	47	43
T3	19.3	20.5	1.8	1.7	53	53

[a] Determined by elemental analysis.
[b] Determined by ^{29}Si MAS NMR spectroscopy.
[c] Calculated from ^{27}Al MAS NMR signal loss.

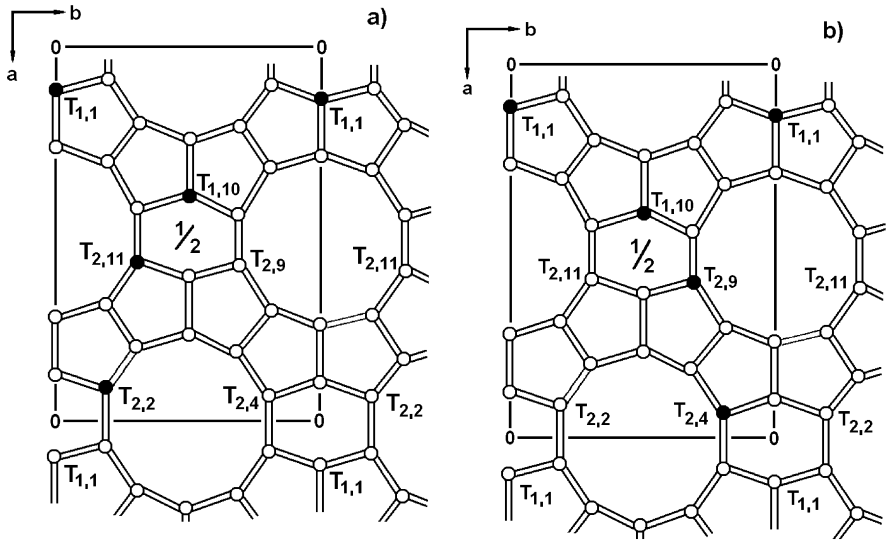

Scheme 2. Model of the distribution of Al atoms (4 Al per unit cell) in the FER framework, following the Takaishi et al. paper [28].

The ^{29}Si MAS NMR spectra of the reference sample T0 and the dealuminated FER materials were deconvoluted using the aforementioned line positions. Analysis of the deconvoluted spectra indicates that framework aluminum atoms located in the vicinity of silicon atoms at T_B positions (Figs. 2b–2e) are preferentially depleted during the dealumination process. These T_B positions contribute to the 10-membered oxygen rings of the zeolite main channels. Thus it can be concluded that the aluminum atoms located in the vicinity of Si(1Al) T_A sites are much more resistant to dealumination. Such a behavior is probably because of their hidden location exclusively in the five- and six-membered oxygen rings of the zeolite structure and thus decreased accessibility for attack by hydrochloric acid, and/or higher stability of such sites in the zeolite framework.

In Table 2, columns 2 and 3, the framework n_{Si}/n_{Al} ratios of the materials under study as determined by ^{29}Si MAS NMR spectroscopy are compared with the results of the elemental analysis. As evidenced by the quantitative evaluation of the ^{29}Si MAS NMR spectra (Fig. 2 and Table 2, last column), up to 53% of the initial aluminum atoms were removed from the FER framework by the treatment with hydrochloric acid solutions. Dealumination of the FER crystals corresponds to a change in the n_{Si}/n_{Al} framework ratio from the initial value of 9.1 to the final value of 20.5 after the final dealumination step. This is a substantially higher increase in the framework n_{Si}/n_{Al} ratio compared with those achieved in earlier attempts based on the zeolite treatment with, for example, ammonium hexafluorosilicate [30].

^{1}H MAS NMR investigations were performed to gain quantitative insight into the distribution and amount of the OH groupings. The spectrum of the reference sample T0 consists of two lines with chemical shifts of 1.8 and 4.2 ppm, which were assigned to the isolated silanol groups and the bridging OH groups (SiOHAl) acting as Brønsted acid sites in the FER framework, respectively (Fig. 3) [31]. After dealumination of T0, a new signal appeared at 2.8 ppm, the intensity of which increased further on treatment with HCl. This signal is due to hydroxyl groups bound to the extra-framework aluminum species (AlOH) [32]. Such species give rise to Lewis acidity. An additional signal at ca. 6 ppm indicated the occurrence of SiOH groups, which are hydrogen-bonded to neighboring oxygen atoms [33]. The ^{1}H MAS NMR signal at 2.8 ppm indicated that some of the aluminum atoms, depleted from the zeolite framework positions, remained in the channels; that is, they were not extracted from zeolite particles by the aqueous solution of hydrochloric acid. This observation was confirmed by ^{27}Al MAS NMR, where the spectra of the dealuminated samples T1–T3 exhibited a signal at ca. 0 ppm attributed to extra-framework aluminum species (Fig. 1).

Table 3
Concentration and strength of Brønsted acid sites in parent T0 (H-FER) and dealuminated ferrierite samples (T1 and T3)

Sample	ν_{OH} (cm^{-1})	Concentration of Brønsted acid sites (mmol/g)			Strength of acid sites [b]	
		^{1}H MAS NMR [a]	FT IR [b]	Average	A_{650}/A_0	$\Delta\nu_{OH}$ [c] (cm^{-1})
T0 (H-FER)	3603	1.389	1.182	1.29	0.29	286
T1	3603	0.986	0.845	0.92	0.45	291
T3	3604	0.380	0.260	0.32	0.51	299

[a] Determined by ^{1}H MAS NMR spectroscopy.
[b] Using ammonia and extinction coefficient 14.8 cm/μmol [34].
[c] Shift observed after CO adsorption.

The intensities of the ^{1}H MAS NMR signals at 4.2 ppm were used to calculate the concentration of SiOHAl groups (exhibiting Brønsted acidity) in the FER samples. The results are listed in Table 3, column 3. The results can be compared with expected amount of acid sites for the T0 sample, equal to 1.67 mmol H^+/g. Interestingly, the concentration of Brønsted acid centers in the dealuminated FER samples is significantly lower than that of the tetrahedrally coordinated framework aluminum atoms (compare Table 3, column 3, and Table 2, columns 4 and 5). This points to a compensation of some of the negatively charged framework aluminum tetrahedra $[AlO_4]^-$ by cationic extra-framework aluminum species.

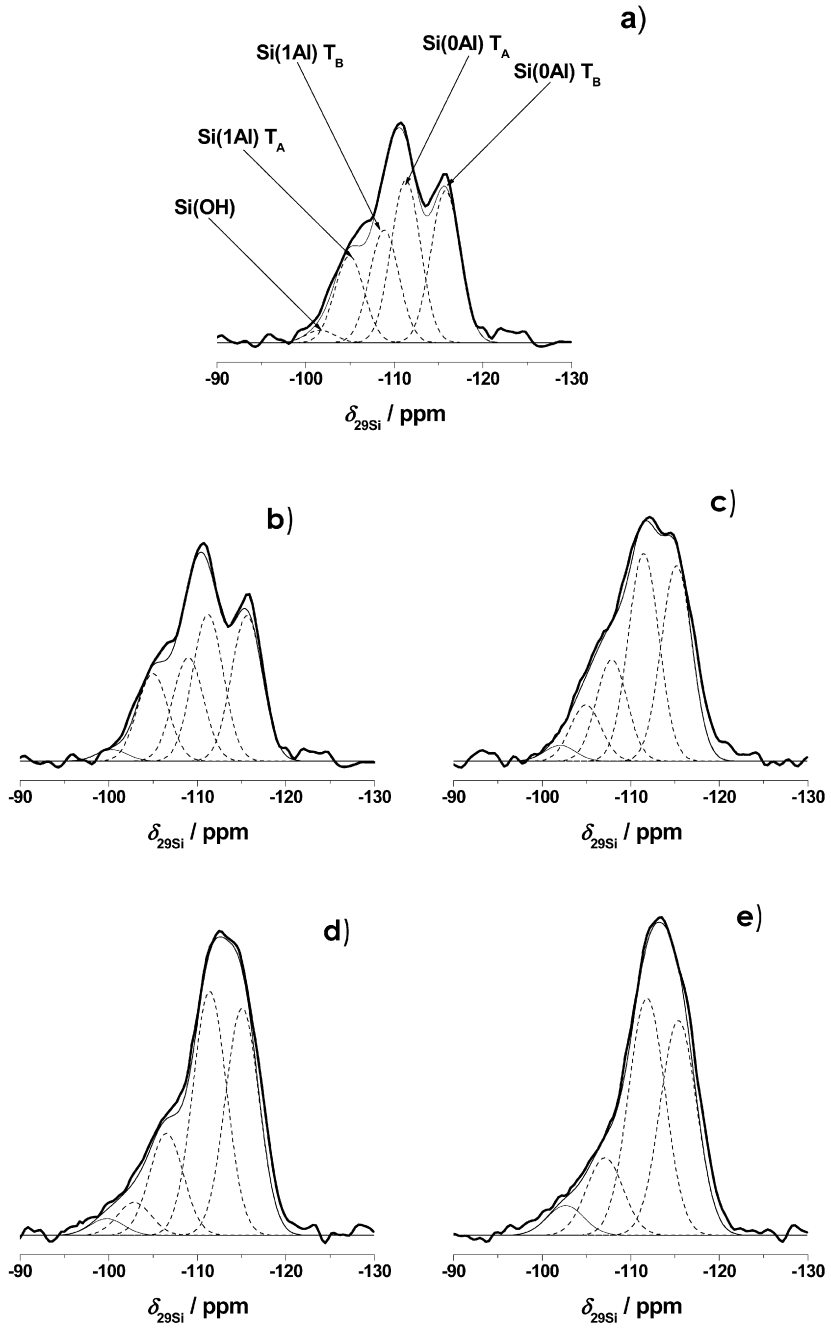

Fig. 2. ^{29}Si MAS NMR spectra of the parent zeolite NH_4-T (a), the reference catalyst T0 (b), and the dealuminated samples T1–T3 (c–e, respectively).

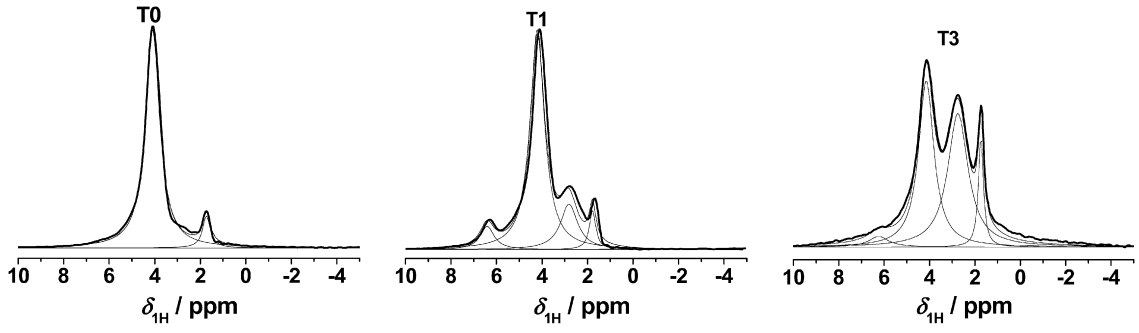

Fig. 3. ^{1}H MAS NMR spectra of dehydrated zeolites T0, T1, and T3.

As expected, the average concentration of Brønsted acid sites decreases on dealumination, from 1.29 to 0.32 mmol H^+/g.

FTIR spectroscopy was applied as a complementary tool for characterizing the hydroxyl coverage of the FER zeolites under study. The spectrum of the dehydrated zeolite T0 (H-FER) consists of two distinct bands at 3748 and 3603 cm^{-1}, a very small band at 3650 cm^{-1}, and a shoulder at 3550 cm^{-1} (Fig. 4). The band at 3748 cm^{-1} corresponds to the terminal SiOH. According to Datka et al. [34], the bands near 3600 and 3550 cm^{-1} are due to bridging SiOHAl groups located inside 10-membered ring channels and inside FER cages, respectively. The position of the main OH band essentially does not change on dealumination (Table 3).

The additional band at 3650 cm^{-1}, barely seen in T0, increased after treatment with HCl (Fig. 4, sample T3). Simultaneously, a significant decrease of the main peak at 3604 cm^{-1} occurs. Peixoto et al. [35] showed that the band at 3650 cm^{-1} in the FTIR spectra of FER zeolites could be related to hydroxyl groups bound to extra-framework aluminum species. In present work, this explanation is supported by the ^{27}Al MAS NMR signals of the octahedrally coordinated extra-framework aluminum species in the samples T1–T3 (Fig. 1). In addition, the ^{1}H MAS NMR spectra of dealuminated samples (Fig. 3) revealed a signal at 2.8 ppm, assigned to the AlOH groups formed at extra-framework aluminum species.

Finally, the strength of the SiOHAl acid sites was estimated by thermodesorption of ammonia and shifts of the OH stretching vibrations on adsorption of CO. Both methods indicated an increasing strength of the Brønsted acid sites on dealumination with HCl (Table 3), similar to that seen for other zeolites [22].

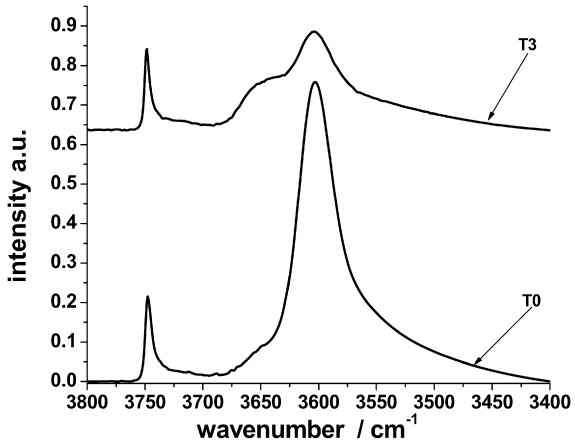

Fig. 4. FTIR spectra of dehydrated zeolites T0 and T3.

3.2. Isomerization of α-pinene

Isomerization of α-pinene can proceed by two parallel routes, one giving rise to the formation of monocyclic products exemplified by limonene, terpinenes, terpinolene, and *p*-cymene, and the other yielding bicyclic and tricyclic products, of which camphene is the most important (Scheme 3). The first step in the reaction involves protonation of the double bond giving the pinanyl cation. The second involves a Wagner–Meerwein-type rearrangement leading to isobornyl and *p*-menthenyl cations. Further rearrangements of isobornyl cations yield camphene and other bicyclic and tricyclic products. In contrast, *p*-menthenyl cations are transformed into limonene, *p*-cymene, and other monocyclic compounds.

Fig. 5 shows the conversion of α-pinene as a function of time at 363 K. The main products obtained are camphene, limonene,

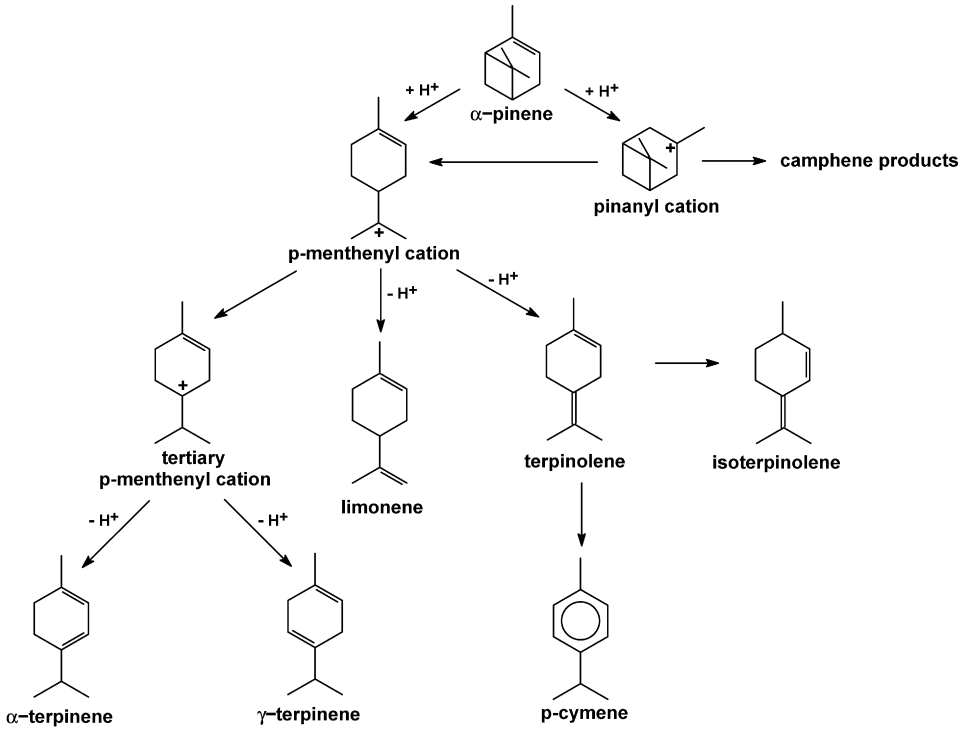

Scheme 3. Mechanism of the α-pinene isomerization.

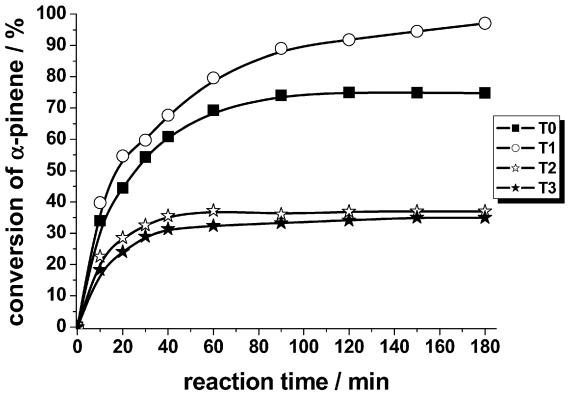

Fig. 5. Conversion of α-pinene vs the reaction time for the isomerization reaction on the reference zeolite T0 and the dealuminated catalysts T1–T3.

Table 4
Comparison of the initial rate of α-pinene transformation on ferrierite type (T0–T3), 12-tungstophosphoric acid (HPW)/SiO_2 and H_2SO_4/ZrO_2 systems

Sample	Acidity (mmol H^+/g)	Initial reaction rate, r_0 (mmol α-pinene/(g_{cat} min))	Reference
T0	1.29	4.28	This work [a]
T1	0.92	5.01	
T2	–	2.82	
T3	0.32	2.31	
HPW/SiO_2-200	1.63	0.63 [b]	[13]
HPW/SiO_2-300	2.15	0.95 [b]	
HPW/SiO_2-400	2.85	1.42 [b]	
15% H_2SO_4/ZrO_2			[14b]
SZ	0.24 [c]	1.47 [d]	
SZ250	0.20 [c]	1.53 [d]	

[a] Reaction temperature 363 K.
[b] Reaction temperature 333 K, calculated from data in Ref. [13].
[c] Expressed in mg of pyridine desorbed.
[d] Reaction temperature 393 K, calculated from data in Ref. [14b].

α- and γ-terpinene, terpinolene, and p-cymene. As seen, the conversion of α-pinene for all of the catalysts studied increased at the beginning and continued to increase with time of the reaction. The conversion of α-pinene on the hydrogen form of FER approached 70% after 3 h. The catalytic performance of the sample T1 (after the first dealumination step) was the best, resulting in ca. 97% conversion of α-pinene. For the other samples, the conversion leveled up after 1 h (Fig. 5).

Dealumination of FER affected the initial rate of α-pinene transformation (Table 4). The first dealumination step seemed to be the most important for the course of the reaction. During this step, ca. 1 Al was removed from the unit cell of FER, while simultaneously the most significant increase in acid strength occurred (i.e., parameter A650/A0 increased from 0.29 to 0.45; Table 3). The initial reaction rate, r_0, was highest for the sample T1 after the first dealumination step, and then decreased significantly on further depletion of aluminum from the FER framework (Table 4).

Further dealumination of FER is detrimental both for the initial reaction rate and for the final conversion achieved, not exceeding ~35% after 3 h (Fig. 5). Thus, samples T2 and T3 were significantly less active than the reference sample T0 and dealuminated sample T1. As is evident from Table 3, while a large decrease in the acid centers occurred for T3, their strength grew only slightly. Advanced dealumination, despite producing a pronounced system of mesopores in the samples (Table 1), facilitating transport of the reaction products, is not optimal for the course of the reaction studied. Clearly, an optimum between the amount of acid centers and their strength is needed to give good catalytic performance. Such observations were described earlier for ZSM-5 [36] and mordenite [37]. In the former case, an optimum amount of Brønsted and Lewis acid sites, as determined by ^1H and ^{27}Al MAS NMR spectroscopy, is required to achieve maximum catalytic activity in n-hexane cracking over dealuminated ZSM-5 [36]. Similarly, ethylbenzene conversion plotted against the Si/Al ratio in mordenite passes through a maximum [37]. In conclusion, dealumination of FER is a favorable method for preparation of zeolitic catalysts, because both the number and the strength of acid centers may be affected by the HCl treatment [22].

It also seems that extra-framework aluminum plays a non-negligible role in catalysis. These species, directly evidenced by ^1H and ^{27}Al MAS NMR, barely existing in the parent hydrogen form T0, appear after the first dealumination step (sample T1, Figs. 1 and 3), giving rise to the Lewis-type centers. These are known to possibly interact with the Brønsted acid sites, enhancing their strength. Moreover, dealumination changes the proportion between the two kinds of acid centers, and the Lewis centers become significant when dealumination is advanced (Figs. 3b and 3c). For such samples (i.e., T2 and T3), lower conversion of α-pinene was found. The small amount of relatively strong acid centers (25% in T3 compared with T0) might be effectively poisoned by heavier reaction products, leading to stable conversion after 40–60 min (Fig. 5). Such site poisoning was considered by López et al. [10].

Moreover, it has been observed in other systems (e.g., H_2SO_4/ZrO_2) that if only Lewis acid sites are present, then no catalytic activity is evidenced, whereas pure Brønsted acidity leads to low overall activity [14b]. The best catalytic performance in the isomerization of α-pinene on H_2SO_4/ZrO_2 was demonstrated for catalysts having both Brønsted and Lewis acid centers.

Generally, camphene and limonene are the main reaction products of the conversion of α-pinene on FER catalysts. The selectivity toward these compounds was close to 85% for all the materials studied. The selectivity to camphene for zeolite T0 was 52% (Fig. 6a); simultaneously, the selectivity of limonene formation was 35% (Fig. 6b). As can be seen from Fig. 6, the selectivity toward camphene and limonene remained almost the same with increasing reaction time, in contrast to the results of Severino et al. [3]. This difference might be attributed to a very dissimilar structure of the faujasite and FER-type zeolites, as well as a significant difference in the number of OH groups in both materials.

The selectivity toward camphene and limonene in the liquid-phase isomerization of α-pinene was explored as a function of the number of dealumination treatments. Fig. 7 illustrates selectivity toward the main products obtained after a reaction time of 180 min, corresponding to maximum conversion of α-pinene on

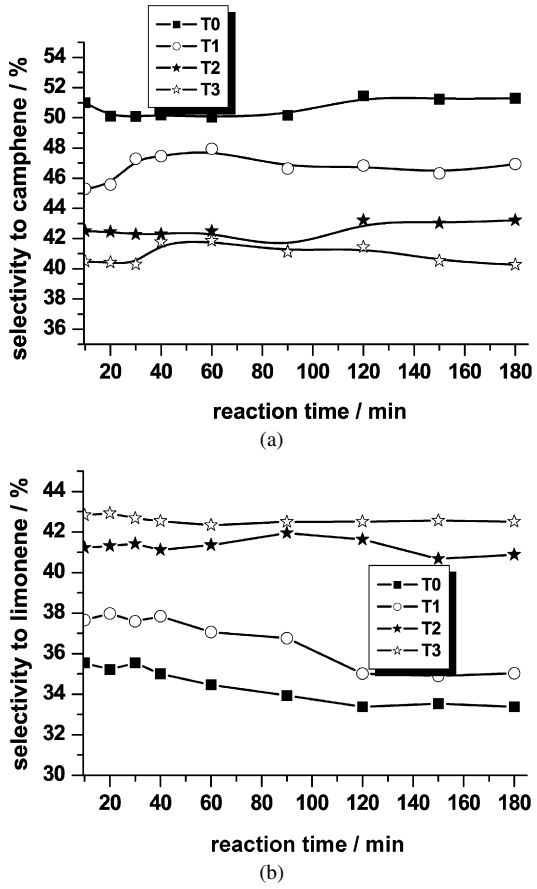

Fig. 6. Selectivity towards camphene (a) and limonene (b) as a function of reaction time.

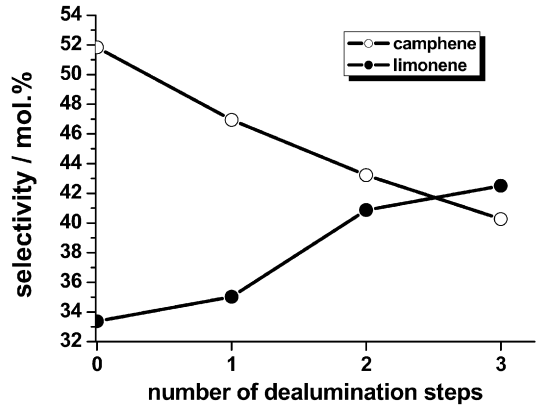

Fig. 7. Selectivity towards camphene and limonene after a reaction time of 180 min vs the number of dealumination steps.

all samples. The selectivity to camphene decreased with each dealumination step, from ca. 52% for the reference material T0 to 41% for the FER zeolite obtained after the third dealumination step. Simultaneously, the selectivity toward limonene increased. Such behavior can be explained by an increased strength of the Brønsted acid sites in the dealuminated FER samples, which favors formation of limonene [3]. Tailoring the reaction parameters (e.g., temperature, α-pinene-to-catalyst ratio) can be expected to produce further improvements in selectivity.

Of interest is the question of where the reaction proceeds, in the internal micropore system or on the external surface of crystallites/mesopores. We note that zeolites often can adsorb molecules having theoretical dimensions somewhat larger than the pore size of the molecular sieve, although the average dimension should not exceed 3 Å [38]. Thus, liquid-phase adsorption of alpha-pinene on ZSM-11 zeolite and its pure-silica homologue Silicalite II was described, with ZSM-11 having a pore dimension of 5.3 × 5.4 Å [19]. Similarly, 1,2,4- and even large 1,3,5-trimethylbenzene can enter the pore system of ZSM-5 [39]. Critical dimensions of these molecules are 7.4 and 8.6 Å, whereas crystallographic dimensions of the larger channel in ZSM-5 are only 5.3 × 5.6 Å [19]. The molecular size of α-pinene is comparable with that of benzene, with corresponding data of 6.63 × 7.74 Å for benzene and 6.77 × 6.91 Å for α-pinene [40]. Benzene, toluene, and xylenes are sorbed in FER pore system [23,24]. Sorption of toluene on FER samples has been reported to be 23–26 mg/g [24], whereas sorption of α-pinene on samples T0 and T3 was much higher (88–109 mg/g).

Furthermore, there is no relationship between mesopore volume and the catalytic activity of the samples. The amount and strength of Brønsted acid centers located inside the zeolite pore systems, together with the presence of Lewis sites in their vicinity, exert such a strong influence on the catalytic activity that it is reasonable to assume that the reaction proceeds mainly inside the micropore system of FER.

Finally, we compared the performance of FER-type materials with that of other systems containing acid centers: 12-tungstophosphoric acid (HPW) supported on SiO_2 and H_2SO_4 supported on ZrO_2. We calculated the initial rate of α-pinene transformations (r_0) over FER catalysts, as well as for the other two systems based on published data [13,14b], and found that the reaction rate of α-pinene over zeolite catalysts was comparable with, and generally higher than those found for the HPW/SiO_2 and H_2SO_4/ZrO_2 systems (Table 4).

4. Conclusion

We have developed a procedure for the dealumination of FER-type zeolite that allows removal of up to 53% of the framework aluminum atoms from the parent material. The procedure involves treatment of the ammonium form of FER (NH_4-T) with aqueous solutions of hydrochloric acid of different concentrations. The dealuminated materials retain their crystallinity and good sorption properties, as demonstrated by nitrogen and α-pinene adsorption studies. NMR and IR spectroscopy studies enabled us to closely follow the course of dealumination of FER and, in particular, the distribution of aluminum in the samples.

^{29}Si MAS NMR spectroscopic studies indicated that the attack of HCl caused selective removal of aluminum atoms located at different crystallographic positions in the FER framework. The framework aluminum atoms were preferentially removed from their positions in the vicinity of silicon atoms occupying T_B sites. These aluminum atoms contributed to the 10-membered oxygen rings of the main channels. In contrast, aluminum atoms, bound via oxygen bridges to silicon atoms at

the T_A positions, were much more resistant to dealumination. The latter are located exclusively in the five- and six-membered oxygen rings of the zeolite structure, which are less prone to attack by hydrochloric acid and possibly more stable.

Even relatively mild dealumination of FER with 0.25 M HCl yielded the catalyst T1 exhibiting 97% conversion of α-pinene at 363 K, compared with the parent hydrogen form of FER, which exhibited only 72% conversion. This sample, containing both Brønsted and Lewis acid centers (with the former predominating), gave the best catalytic performance. When the dealumination level was more advanced, catalytically less active materials were obtained, due to decreased overall acidity and the altered ratio between the Brønsted and Lewis acid centers.

The selectivity toward camphene and limonene was affected by the dealumination level; a greater selectivity toward limonene was observed at the expense of camphene formation with an increasing n_{Si}/n_{Al} ratio of the catalysts. This finding can be explained by the increased strength of Brønsted acid sites on dealumination. The selectivity toward camphene and limonene remained essentially constant during reaction times of up to 180 min. The overall selectivity toward camphene + limonene was close to 85% for all of the FER samples studied.

Finally, we note that the initial rate of α-pinene transformations over FER-type zeolites in the liquid phase is comparable with that of other systems, and generally exceeds that found for the HPW/SiO_2 and H_2SO_4/ZrO_2 catalysts.

Acknowledgments

Financial support was provided by the European Union under a Marie Curie Action grant TOK-CATA (no. MTKD-CT-2004-509832), and by the grant of the Ministry of Science and Higher Education, Warsaw (no. PBZ-KBN-116/T09/2004). The authors thank Professor J. Datka and Dr. K. Góra-Marek of Jagiellonian University, Kraków, for the IR measurements.

References

[1] J.L.F. Monteiro, C.O. Veloso, Top. Catal. 27 (2004) 169.
[2] V.P. Wystrach, L.H. Barnum, M. Garber, J. Am. Chem. Soc. 79 (1957) 5786.
[3] A. Severino, A. Esculcas, J. Rocha, J. Vital, L.S. Lobo, Appl. Catal. A Gen. 142 (1996) 255.
[4] C.M. López, F.J. Machado, K. Rodríguez, B. Méndez, M. Hasegawa, S. Pekerar, Appl. Catal. A Gen. 173 (1998) 75.
[5] M. Gscheidmeier, R. Gutmann, J. Wiesmüller, A. Riedel, US Patent 5,559,127 (1997).
[6] L. Grzona, N. Comelli, O. Masini, E. Ponzi, M. Ponzi, React. Kinet. Catal. Lett. 69 (2) (2000) 271.
[7] M.A. Ecormier, A.F. Lee, K. Wilson, Microporous Mesoporous Mater. 80 (2005) 301.
[8] A.I. Allahverdiev, G. Gündüz, D.Y. Murziny, Ind. Eng. Chem. Res. 37 (1998) 2373.
[9] A. Allahverdiev, S. Irandoust, D.Y. Murzin, J. Catal. 185 (1999) 352.
[10] C.M. López, F.J. Machado, K. Rodríguez, D. Arias, B. Méndez, M. Hasegawa, Catal. Lett. 62 (1999) 221.
[11] D.R. Brown, C.N. Rhodes, Catal. Lett. 45 (1997) 35.
[12] C. Breen, R. Watson, J. Madejova, P. Komadel, Z. Klapyta, Langmuir 13 (1997) 6473.
[13] O. Masini, L. Grzona, N. Comelli, E. Ponzi, M. Ponzi, J. Chil. Chem. Soc. 48 (2003) 101.
[14] (a) N.A. Comelli, L.M. Grzona, O. Masini, E.N. Ponzi, M.I. Ponzi, J. Chil. Chem. Soc. 49 (2004) 245;
(b) N.A. Comelli, E.N. Ponzi, M.I. Ponzi, Proc. 2nd Mercosur Congr. Chem. Eng. & 4th Mercosur Congr. Process Sys. Engng., 14–18.08.2005, Rio de Janeiro, Enpromer 2005.
[15] A.D. Newman, A.F. Lee, K. Wilson, N.A. Young, Catal. Lett. 102 (2005) 45.
[16] R. Ohnischi, K. Tanabe, Chem. Lett. 3 (1974) 207.
[17] A.F. Plate, M.W. Mil'vitskaya, Teknologiya 10 (1967) 1340.
[18] M. Gscheidmeier, H. Häberlein, H.H. Häberlein, J.T. Häberlein, M.C. Häberlein, US Patent 5,826,202 (1998).
[19] Ch. Baerlocher, W.M. Meier, D.H. Olson, Atlas of Zeolite Framework Types, Elsevier, Amsterdam, 2001, http://topaz.ethz.ch/IZA-SC/atlas_pdf/.
[20] B. Sulikowski, Czasop. Techn. 195 (1976) 33.
[21] D.W. Breck, Zeolite Molecular Sieves, Wiley, New York, 1974.
[22] B. Sulikowski, Heterogen. Chem. Rev. 3 (1996) 203.
[23] R. Rachwalik, Z. Olejniczak, B. Sulikowski, Catal. Today 101 (2005) 147.
[24] Y.S. Shin, A. Auroux, J.C. Vedrine, Appl. Catal. 37 (1988) 1 (Part I), 21 (Part II).
[25] J. Klinowski, S. Ramdas, J.M. Thomas, C.A. Fyfe, J.S. Hartman, J. Chem. Soc. Faraday Trans. II 78 (1982) 1025.
[26] P.P. Man, J. Klinowski, A. Trokiner, H. Zanni, P. Papon, Chem. Phys. Lett. 151 (1988) 143.
[27] P.P. Man, J. Klinowski, J. Chem. Soc. Chem. Commun. (1988) 1291.
[28] T. Takaishi, M. Kato, K. Itabashi, Zeolites 15 (1995) 21.
[29] P. Sarv, B. Wichterlová, J. Čejka, J. Phys. Chem. B 102 (1998) 1372.
[30] P. Cañizares, A. Carrero, Appl. Catal. A Gen. 248 (2003) 227.
[31] D. Freude, M. Hunger, H. Pfeifer, G. Scheler, J. Hoffmann, W. Schmitz, Chem. Phys. Lett. 105 (1984) 427.
[32] M. Hunger, Catal. Rev.-Sci. Eng. 39 (1997) 345.
[33] C. Doremieux-Morin, P. Batamack, J.M. Bregeult, J. Fraissard, Catal. Lett. 9 (1991) 403.
[34] J. Datka, M. Kawałek, K. Góra-Marek, Appl. Catal. A Gen. 243 (2003) 293.
[35] D.P.B. Peixoto, S.M. Cabral de Menezes, M.I. Pais da Silva, Mater. Lett. 4451 (2003) 1.
[36] E. Brunner, H. Ernst, D. Freude, M. Hunger, C.B. Krause, D. Prager, W. Reschetilowski, W. Schwieger, K.-H. Bergk, Zeolites 9 (1989) 282.
[37] D. Seddon, Appl. Catal. 7 (1983) 327.
[38] A.E. Comyns, G.W. Morris, J.P. Sankey, US Patent 4,687,871 (1987).
[39] H.P. Röger, K.P. Möller, C.T. O'Connor, Microporous Mater. 8 (1997) 151.
[40] A. Berenguer-Murcia, A.J. Fletcher, J. Garcia-Martinez, D. Cazorla-Amoros, A. Linares-Solano, K.M. Thomas, J. Phys. Chem. B 107 (2003) 1012.